

# A laser diagnostic for HCN detection in mid-infrared

Ali Elkhazraji<sup>1</sup>, Mohammad Adil<sup>1</sup>, Binod Giri<sup>1</sup>, Mhanna Mhanna<sup>1</sup>, Nawaf Abualsaud<sup>1</sup>, Ahmed Ayidh Alsulami<sup>1</sup>, Mohammad Khaled Shakfa<sup>1</sup>, Marco Marangoni<sup>2</sup>, Aamir Farooq<sup>1</sup>

1. Physical Science and Engineering Division, King Abdullah University of Science and Technology (KAUST), Thuwal, 23955, Saudi Arabia

2. Department of Physics and IFN-CNR, Politecnico di Milano, Via G. Previati 1/C, 23900 Lecco, Italy

Author e-mail address: aamir.farooq@kaust.edu.sa

**Abstract:** A difference-frequency generation (DFG) laser is used to develop a diagnostic for HCN sensing near 14  $\mu\text{m}$ . Pressure- and temperature-dependent absorption cross-sections are reported. The sensor is showcased in shock tube chemical kinetic experiments. © 2022 The Author(s)

## 1. Introduction

Laser-based diagnostics have been a powerful tool to employ in combustion research and chemical kinetic studies as they offer in-situ, time-resolved, nonintrusive measurements, e.g., species formation time-histories. Particularly, laser absorption spectroscopy in the mid-infrared (MIR) provides species-specific, sensitive measurements of many hydrocarbons since they possess strong absorption features in the MIR. Although access to MIR has been facilitated by recent advances in laser technology, laser availability in the long-wavelength MIR region ( $> 13 \mu\text{m}$ ) is still limited. Sensing hydrogen cyanide (HCN) at high temperatures is of high interest, since HCN is one of the main  $\text{NO}_x$  precursors in combustion systems. However, only a few suitable techniques enable measuring HCN accurately [1]. The strong  $\nu_2$  vibrational band of HCN lies near 14  $\mu\text{m}$  which makes it difficult to probe using commercially available lasers. This band is favorable for HCN detection for several reasons, including: 1) it is the strongest MIR band of HCN, 2) it lies in the molecular fingerprint spectral region which offers better selectivity, and 3) hot band transitions of HCN near 14  $\mu\text{m}$  enhance sensitivity at higher temperatures. Herein, we report a tunable laser sensor for HCN, probing its  $\nu_2$  band based on a DFG process between a  $\text{CO}_2$  gas laser and external-cavity quantum cascade laser (EC-QCL).

## 2. Sensor Description

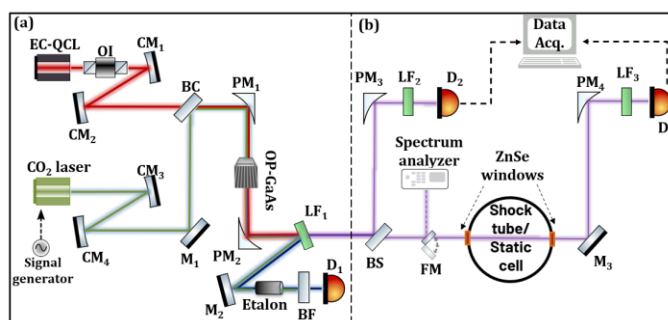


Fig. 1. Schematic of (a) the DFG laser setup and (b) the shock tube and related optics. OI: optical isolator; CM: concave mirror; BC: beam combiner; PM: parabolic mirror; M: flat mirror; OP-GaAs: orientation-patterned GaAs crystal; LF: long-pass filter; BF: band-pass filter; D: detector; BS: beam splitter; FM: flip mirror.

Figure 1(a) shows a schematic of the difference-frequency generation (DFG) laser setup. The DFG process is carried out in a nonlinear orientation-patterned gallium arsenide crystal between a continuous wave EC-QCL tunable over  $1750 - 1820 \text{ cm}^{-1}$  and a pulsed  $\text{CO}_2$  gas laser tunable over  $921 - 1083 \text{ cm}^{-1}$ , which results in an idler beam tunable over  $667 - 865 \text{ cm}^{-1}$ . A long-pass filter was placed after the crystal to allow only the idler beam to transmit to the shock tube. A reflected beam of EC-QCL was passed through a germanium etalon to calibrate the DFG wavelength for spectrum scan measurements. Further details about the DFG setup can be found in [2]. A beam splitter was used to split the DFG beam into two branches: one was focused onto a reference detector ( $\text{D}_2$ ,  $\text{HgCdTe}$ ) using a parabolic mirror and the other beam was guided through ZnSe windows, fixed on the shock tube, and was focused onto another detector ( $\text{D}_3$ , see Fig. 1(b)). A spectrum analyzer (Bristol 721B) was used to monitor the wavelengths of the EC-QCL and  $\text{CO}_2$  gas laser. Long pass filters,  $\text{LF}_2$  and  $\text{LF}_3$ , were used to minimize the effect of thermal radiation caused by the shock-heated gasses on the detected signal. A stainless-steel low-pressure shock tube (inner diameter = 14.22 cm) was used to carry out temperature-dependent and reactive experiments. More details about the shock tube facility can be found in [3]. For the pressure-dependent absorption cross-section measurements, the shock tube arrangement was replaced with a 50-cm static cell where the partial pressure of HCN was varied in a nitrogen bath gas.

### 3. Results and Discussion

For shock tube experiments, the DFG wavelength was set to  $\sim 714.5 \text{ cm}^{-1}$  which corresponds to the highest MIR absorption peak at high temperatures ( $> 800 \text{ K}$ ) [4]. Beer-Lambert relation was used to calculate the absorption cross-sections ( $\sigma$ ) and concentrations. Figure 2(a) shows the measured absorbance across the Q-branch of the  $\nu_2$  band of HCN at various pressures to showcase the sensor tunability. Figure 2(b) shows the absorption cross-sections as a function of pressure at the target wavenumber of  $714.5 \text{ cm}^{-1}$ . It is evident that the pressure dependency becomes weak as the pressure approaches 1 bar.

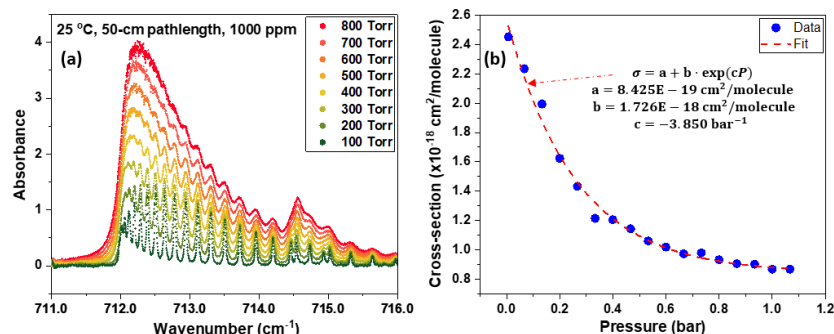


Fig. 2. (a): Absorbance spectrum of the Q-branch for different pressure values; (b): pressure-dependent absorption cross-section at  $714.5 \text{ cm}^{-1}$ .

Figure 3(a) shows temperature-dependent absorption cross-section measurements of HCN (5000 ppm HCN balanced by Ar) behind reflected shocks at varying pressures (0.7–1.3 bar) which confirms the weak pressure dependency as all data points follow the fitted trend regardless of the pressure. The fitted exponential relation was used as an input in the analysis of the reactive experiments to calculate HCN concentration time-histories at a given reflected shock temperature ( $T_s$ ). In these experiments, HCN was produced from isoxazole thermal decomposition (2%  $\text{C}_3\text{H}_3\text{NO}/98\%$  Ar) behind reflected shocks, as shown in Fig. 3(b). Time zero corresponds to the arrival of the shock wave at the measurement location (2 cm from end-wall). We compared our results with simulations using the model proposed in [5], which were in good agreement at relatively long reaction times.

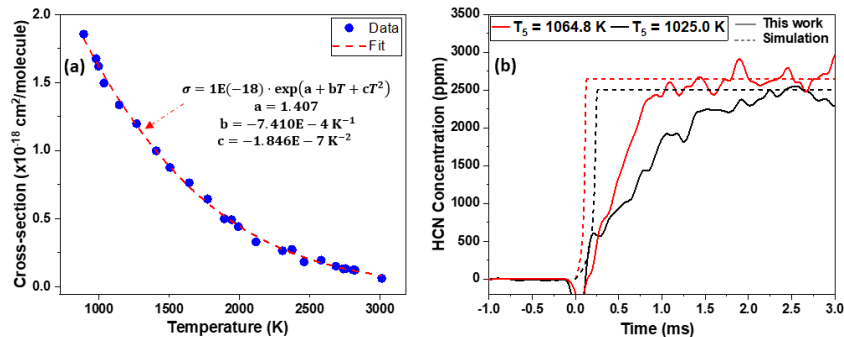


Fig. 3. (a): Temperature-dependent absorption cross-section at  $714.5 \text{ cm}^{-1}$ ; (b): HCN time history in  $\text{C}_3\text{H}_3\text{NO}$  pyrolysis behind reflected shocks.

### 4. Summary

We report a laser-based combustion diagnostic for HCN detection based on a DFG laser emitting at  $714.5 \text{ cm}^{-1}$ . The measured temperature-dependent absorption cross-sections were found to be weakly dependent on pressure and were used to calculate HCN concentration time histories formed by the thermal decomposition of isoxazole in a shock tube.

### 5. References

- [1] M. Stühr, S. Hesse, and G. Friedrichs, "Quantitative and Sensitive Mid-Infrared Frequency Modulation Detection of HCN behind Shock Waves," *Fuels*, vol. 2, no. 4, pp. 437–447, 2021, doi: 10.3390/fuels2040025.
- [2] M. K. Shakfa *et al.*, "A widely tunable difference-frequency-generation laser for high-resolution spectroscopy in the 667–865  $\text{cm}^{-1}$  range," in *Proc.SPIE*, Mar. 2021, vol. 11670, doi: 10.1117/12.2577534.
- [3] S. M. Sarathy *et al.*, "A comprehensive combustion chemistry study of 2,5-dimethylhexane," *Combustion and Flame*, vol. 161, no. 6, pp. 1444–1459, 2014, doi: <https://doi.org/10.1016/j.combustflame.2013.12.010>.
- [4] I. E. Gordon *et al.*, "The HITRAN2020 molecular spectroscopic database," *Journal of Quantitative Spectroscopy and Radiative Transfer*, vol. 277, p. 107949, 2022, doi: <https://doi.org/10.1016/j.jqsrt.2021.107949>.
- [5] A. Lifshitz and D. Wohlfeiler, "Thermal decomposition of isoxazole. Experimental and modeling study," *Journal of Physical Chemistry*, vol. 96, no. 11, pp. 4505–4515, 1992, doi: 10.1021/j100190a070.